参赛队员姓名： 孙博文

中学： 北京市第五中学

省份： 北京

国家/地区： 中国

指导教师姓名： 黄雅钦

指导教师单位： 北京化工大学

论文题目：一种自清洁可复活的无机纤维口罩

An Inorganic Fiber-based Mask with Self-cleaning and Rejuvenation Capability

Author: SUN Bowen

Instructor: HUANG Yaqin

@Beijing University of Chemical Technology

Subject: Chemistry

School: Beijing No.5 High School

City: Beijing, P. R. China

2023-09-14

Contents

Abstract

To reduce the “white” pollution caused by polymer (organic) masks in daily life and medical usage, this subject aims to develop a Nb-TiO_2 (Niobium doped Titania) modified self-cleaning mask with rejuvenation capability based on inorganic glass fiber paper. The mask uses glass fiber as the porous filter materials, to remove sprays containing bacteria or virus. The surface of mask is covered by titanium dioxide nano-particles, which endow the surface with photocatalytic property to mineralize the surface organic pollutants, to achieve self-cleaning effect. Nb-doping was used to promote its photocatalysis efficiency. Different gel solution formula and coating conditions are tried to optimize the filtration and loading effects. The inorganic nature of the mask makes the membrane able to be rejuvenated by baking in high temperature after usage, to achieve recycled utilization. Polymeric framework instead of traditional elastic tapes is used to make the inorganic film easy to replace.

Keywords: Masks, Glass Fiber Membrane, Titanium Dioxide, Photocatalysis, Self-Cleaning

1 Introduction

1.1 Background and Motivation

Since the outbreak of the COVID-19 pandemic, the Centers for Disease Control and Prevention (CDC) in the United States has strongly recommended the use of personal protective equipment (PPE) for self-protection. As an essential component of individual hygiene and health protection in daily life, masks have become the primary focus of production for hygiene and safety purposes[1-2]. However, the majority of medical masks, which have the highest production volume, are composed of a structure known as SMS (Spunbond-Meltblown-Spunbond), with polypropylene (PP) melt blown fabric serving as the main filtering material, accounting for over 90% of the raw materials used [3-4]. This type of fiber fabric offers advantages such as excellent flexibility, strong chemical stability, and high dust electrostatic adsorption capacity. However, its chemical stability also results in difficulties in biodegradation, leading to environmental pollution [5-6]. Polypropylene can be broken down into nano plastics in water, which can easily be ingested by marine organisms. Considering the current World Health Organization recommendation of replacing masks every 3-5 hours, the usage and disposal rates of masks are alarmingly high, resulting in significant pollution

and severe environmental issues (Figure 1). According to a report by the Asian Marine Organization in December 2020, approximately 52 billion masks were produced globally in 2020, and at least 1.56 billion masks were discarded [7]. These discarded masks equate to generating between 4,680 to 6,240 tons of plastic waste, which either ends up in the ocean or gets buried in landfills. Additionally, data shows that with the rapid economic development in China, there has been an increasing demand for various chemical raw materials, leading to the highest consumption level of polypropylene in history. China may become the largest consumer of polypropylene in the world.

Despite the slowing down of the COVID-19 pandemic, medical masks remain an essential item for daily use by healthcare workers. According to the World Health Organization's estimation, global healthcare workers alone consume around 89 million surgical masks per month, and these discarded masks will continue to pollute the marine and terrestrial ecosystems in the long term. The issue of mask pollution has prompted us to rethink the current usage pattern. Developing a self-cleaning and renewable mask that can be reused through specific treatment processes would significantly reduce the environmental pollution caused by masks.

In this study, to address the plastic pollution associated with used masks, we developed a self-cleaning mask with rejuvenation capability by incorporating Nb-TiO_2 modification into an inorganic glass fiber paper-based structure. The mask utilizes glass fiber as a porous filter material to effectively capture sprays containing bacteria or viruses. The surface of the mask is coated with titanium dioxide nanoparticles, which confer photocatalytic properties for the mineralization of surface organic pollutants, thereby achieving a self-cleaning effect. Nb-doping is employed to enhance the photocatalytic efficiency of the mask. Various formulations of gel solutions and coating conditions are experimented to optimize filtration and loading effects. The inorganic nature of the mask allows for rejuvenation through baking at 450°C after use, facilitating its recyclability. To ensure ease of replacement, a polymeric framework is utilized instead of traditional elastic tapes for the inorganic film.

Figure 1 Marine pollution (left) and retention (right) caused by abandoned face masks

1.2 Current Study on Inorganic Fiber Papers

In contrast to organic cotton using in masks, rocks can also be centrifugally blown into artificial inorganic fibers under high-temperature melting conditions [8]. In nature, there exists a type of mineral cotton formed from igneous rocks, primarily composed of basalt or diabase, with chemical constituents such as silica dioxide, calcium oxide, and aluminum oxide.

Similarly, glass fiber is an inorganic, non-metallic material made from glass, characterized by outstanding physical and chemical properties, including high strength, heat resistance, and corrosion resistance. It is predominantly used as a reinforcement material in applications such as Glass Fiber Reinforced Plastics (GFRP) and Glass Fiber Reinforced Concrete (GFRC) [9,10]. Furthermore, glass fibers find applications in various fields, including electronics, telecommunications, optical fiber transmission, and aerospace.

Both glass fibers and rock cotton share porous and high-temperature-resistant (>400°C) characteristics. The porosity can be employed for filtration purposes, while the high-temperature resistance allows for sterilization through heat. Therefore, considering the advantages outlined, the adoption of glass fibers as both the filtration and support layers for masks can be contemplated.

1.3 Current Study on Titanium Dioxide Photocatalysis

Titanium dioxide (TiO_2) has garnered significant attention due to its numerous advantages, including high photocatalytic activity, strong oxidation capability, non-toxicity, and excellent chemical stability. With the development of relevant studies, in recent years, from the perspective of biological applications, many experts have extended the research field of TiO_2 photocatalysis to the category of biological organisms, exploring the spontaneous oxidative destruction of cell (bacterial) tissues, cell membranes, etc. The significance of research in this field is not only to find new types of photocatalytic decomposition of contaminated objects (such as bacteria, viruses, algae and other organic organisms), but also to kill cancer cells (including HIV) or better spontaneous bactericidal ingredients and other research to produce new discoveries.

It has been observed that variations in the size, shape, and crystal structure of TiO_2 nanomaterials not only influence the surface stability of TiO_2 but also exhibit size-dependent transitions between different TiO_2 phases under pressure or heat. Given that many applications of TiO_2 nanomaterials are intimately linked to their optical and catalytic properties, this project primarily focuses on research related to enhancing the optical properties of TiO_2 nanomaterials, including doping and

nano structuring.

As for the photocatalysis principles, titanium dioxide is a wide band gap N-type semiconductor, doping, defects, can cause the increase of electron concentration in the conduction band. When the impurity atom replaces the titanium atom in the lattice in the form of band substitution, it can provide an excess (free) electron in addition to meeting the covalent bond coordination, and this electron enters the conduction band, forming an increase in the concentration of conduction band electrons in the semiconductor, thus promoting the generation of electronic conductivity. Its Fermi level is near the bottom of the conduction band, and the concentration of free electrons is large (conduction band), and the oxide is strong conductance. The band structure of titanium dioxide is generally composed of a low energy valence band (VB) and a high energy conduction band (CB), in which the valence band is filled with electrons and the conduction band is empty, and there is a band gap between the lowest conduction band and the highest energy difference of the valence band. The difficulty of the electrons being excited from the valence band to the conduction band becomes difficult with the increase of the span of the band gap (that is, the energy span), which also leads to the reduction of the intrinsic carrier concentration and the conductivity.

1.3.1 Tauc Plot Principle

This test method is mainly used to measure the absorption coefficient through the relationship between the light absorption threshold and the band gap width. The principle is based on the formula proposed by Tauc et al.

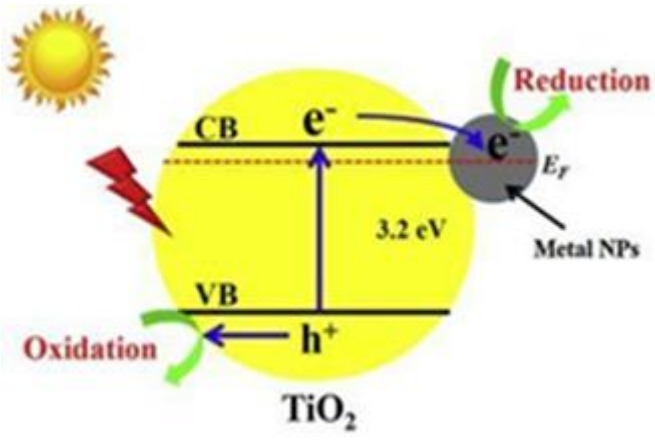

Figure 3. Schematic diagram of TiO_2 photocatalysis

First and foremost, it is essential to elucidate the distinction between direct bandgap semiconductors and indirect bandgap semiconductors. In direct bandgap semiconductors, the

minimum energy of the conduction band (located at the bottom of the conduction band) and the maximum energy of the valence band coincide in k-space. This characteristic results in high radiative recombination efficiency, leading to superior light-emitting properties. Conversely, indirect bandgap semiconductors exhibit a misalignment between the minimum energy of the conduction band and the maximum energy of the valence band, positioning them at different locations in k-space.

When there is a certain frequency of light shining on the semiconductor, the photon energy will cause the semiconductor electrons and holes to separate, forming photogenerated charge carriers, which include electrons and holes. Whether it is N-type or P-type semiconductor, most of its valence band electrons and conduction band electrons are distributed near the band gap, so when the energy is close to the band gap width, a large number of electrons can produce electronic transition by absorbing the energy brought by photons, forming photogenerated electrons (e-). At this time, the absorption coefficient will increase with the increase of the substituted energy, that is, the number of photons.

For semiconductor materials, the following relationship exists between their optical band gap and absorption coefficient:

$$(\alpha h\upsilon)^{\frac{1}{n}}=B(h\upsilon-E_g)$$

Where, α is the absorption coefficient, hν is the photon energy, h is Planck's constant ($h\approx4.13567\times10^{-15}$ eV·s), ν is the incident photon frequency (ν=c/λ, where c is the speed of light $\approx3\times10^{8}$ m/s; λ is the wavelength of the incident light), B is the proportionality constant, and E_g is the band gap width of the semiconductor material. The value of n is related to the type of semiconductor material, when the semiconductor material is a direct band gap, n=1/2; n=2 when the semiconductor material has an indirect band gap. By the above means, combine with the following formula:

$$E_g=\frac{1240}{\lambda g}$$

In this formula, where λg is measured in nanometers (nm) and Eg is expressed in electronvolts (eV), it is believed that the band edge wavelength (λg) of a semiconductor is intrinsically linked to its band gap width (Eg). Meanwhile, Eg can be deduced by considering the value of λg. It is important to note that the absorption wavelength threshold for commonly employed wide band gap semiconductors predominantly falls within the ultraviolet spectrum, typically lacking significant

absorption of visible light.

1.3.2 Photocatalytic Mechanism of TiO_2

The mechanism of TiO_2 photocatalysis is that electrons in valence band are excited to conduction band by photon energy much larger than their own energy, which generates electron (e^-) and creates hole (h^+) at the same time, thus triggering two possible processes of recombination or separation.

Under the action of electric potential field, electron (e^-) and hole (h^+) will rapidly combine under strong energy. The equation is as follows:

$$TiO_2+hv\rightarrow h^+ + e^-$$

Under the action of potential field, the two will be separated by migration to the conduction band and valence band surface, the hole has strong oxidation, the electron has strong reducibility.

The reaction equation is as follows:

$$O_2+ e^-\rightarrow O_2^-$$

$$2O_2^-+2H_2O\rightarrow 2H_2O_2+O_2$$

$$H_2O_2+O_2\rightarrow \cdot OH+ H^+ +O_2$$

$$2H_2O_2+e^-\rightarrow \cdot OH+OH^-$$

In the above process, the following reaction will occur with respect to the hole:

$$h^++OH^-\rightarrow \cdot OH$$

$$h^++H_2O\rightarrow \cdot OH+H^+$$

$$h^++e^-\rightarrow \cdot \text{thermal energy}$$

It can be seen that the photocatalytic reaction of titanium dioxide is essentially a free radical reaction. As the intermediate and result products, ·OH and O^{2-} are highly oxidizing (·OH oxidation potential is 2.8V, superoxide anion as an anion is a free radical, active and easy to disproportionate). Most organic pollutants (including but not limited to bacteria, viruses, etc., under ultraviolet environment in the air) can be mineralized into inorganic small molecules in the photocatalytic process, such as carbon dioxide and water, etc. which is mainly reflected in the targeted destruction of cell membranes.

1.3.3 Preparation Methods

Regarding the current status of nano-TiO_2 preparation, the primary methods for producing titanium dioxide include the sol-gel method, hydrothermal reaction method, hydrolysis method,

microemulsion method, uniform precipitation method, microwave method, micelle, and reverse micelle method. Among these, the sol-gel method stands out as a widely adopted and well-established approach due to its straightforward process, cost-effectiveness of raw materials, high purity of powder production, and ease of film preparation.

The sol-gel method is a widely employed fabrication technique for various ceramic materials. In a typical sol-gel process, a colloidal suspension or sol is formed through the hydrolysis and polycondensation reactions of precursor species. The precursors play the role of intermediate products in this process and can exist as organo-inorganic complexes or mixtures in a solid-state form, or partially in sol form. As the system gradually polymerizes and solvents are progressively removed, the liquid sol transitions into a solid gel. If the solvent in the wet gel is removed under supercritical conditions, it results in aerogel products with high porosity and low density. In this study, we utilized the sol-gel method to prepare nano-thin film materials and applied them to the surface of glass fibers. Specifically, we synthesized TiO_2 nano-materials through the sol-gel process using a titanium precursor, involving acid-catalyzed alcoholysis of titanium alkoxide followed by condensation reactions to produce the final product.

1.3.4 Crystal Structure of TiO_2 Under Different Conditions

Under the optimal experimental conditions, the TiO_2 gel exhibits a rutile-phase crystalline structure, as depicted in Figure 4. Rutile-phase titanium dioxide possesses a tetragonal crystal structure with excellent crystallinity, a large surface area, and high photocatalytic activity. The bimodal characteristics of the rutile phase are not very pronounced, with the lowest electron density higher than the ground-state electron density. The entire crystal structure exhibits an octahedral coordination.

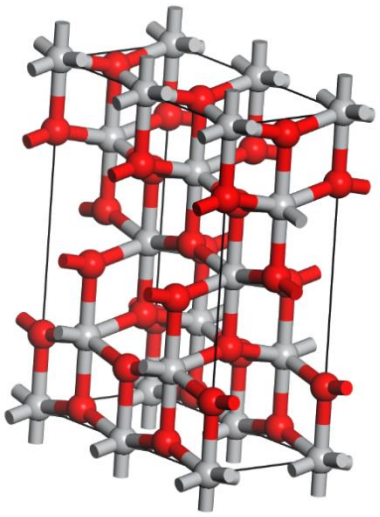

Figure 4. Schematic Diagram of Anatase TiO_2 Crystal Structure

During the calcination process, it is noteworthy that the calcination time and temperature have an impact on the phase transformation of TiO_2 nanomaterials. With increasing temperature and extended calcination times, the TiO_2 nanomaterials gradually crystallize in the dry environment. Simultaneously, the crystalline phase of the nanomaterials shifts from an anatase/rutile structure to a rutile structure, eventually transforming into the tetragonal rutile phase of titanium dioxide, as illustrated in Figure 5.

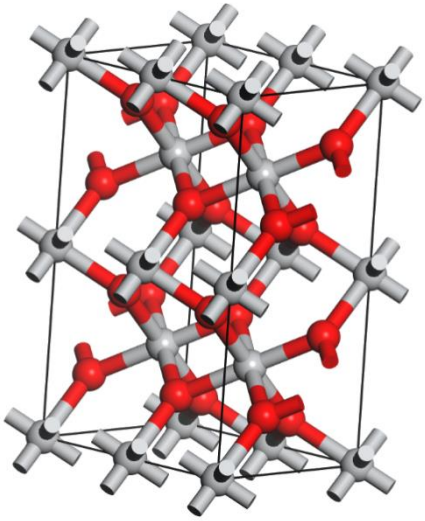

Figure 5. Schematic Diagram of Rutile TiO_2 Crystal Structure

1.4 Design and Main Approach

Glass fibers exhibit both porosity and high-temperature resistance (>400°C). The porosity can be

effectively employed for blocking and filtration purposes, while its high-temperature resistance allows for sterilization through high-temperature methods. Therefore, we are considering the use of glass fibers as the filtration and support layers for a novel inorganic, recyclable face mask.

To achieve room-temperature self-cleaning, we have considered the introduction of a photocatalyst, with titanium dioxide [11-13] being one of the most commonly employed options. Titanium dioxide possesses an electron structure characterized by a full valence band and an empty conduction band. Under ultraviolet irradiation, electron energy reaches or surpasses the band gap energy, facilitating the excitation of valence band electrons in titanium dioxide, thus forming electron-hole pairs. In the presence of an electrostatic field, these electrons and holes become separated and migrate to distinct locations on the surface of titanium dioxide. This process results in the capture of oxygen molecules, leading to the generation of oxygen gas and the production of superoxide anion radicals through reactions with water. These free radicals actively participate in oxidation reactions, attacking organic components within bacterial cell membranes and cytoplasmic matrices. This attack disrupts unsaturated bonds or extracts hydrogen atoms, giving rise to new free radicals, consequently initiating a chain reaction. Ultimately, this chain reaction leads to the decomposition of bacteria, yielding carbon dioxide and water as end products.

Based on these reaction characteristics, we aspire to harness the self-disinfection properties of titanium dioxide in outdoor ultraviolet environments, thereby enabling the sustainable and repetitive use of masks.

Simultaneously, to ensure the comprehensive degradation of organic matter by titanium dioxide, ensuring a low bacterial survival rate and reusability, we consider the robust thermal stability and colorfastness of titanium dioxide at high temperatures. To achieve the intended "long-term sterilization of a mask" and "repeated use," all external mask materials must be inorganic. This choice guarantees that the entire mask can be conveniently subjected to high-temperature cleaning when necessary. Consequently, the main project selection criteria are outlined as follows:

1) Utilization of high-temperature-resistant inorganic glass fiber materials as a framework to establish a porous filter layer capable of regeneration following the adsorption of organic substances.
2) Incorporation of nanometer titanium dioxide photocatalytic sterilization onto the surface of glass fibers, facilitating self-cleaning while in use.

Figure 2. Schematic diagram of the main design ideas of the project: the glass fiber microporous filter membrane is used in the mask, and the surface is loaded with photocatalyst to realize self- cleaning during the wearing process; After long-term use, it can be roasted at high temperature to completely remove bacteria and realize regeneration.

The specific design (as shown in Figure 2) entails using glass fiber as the framework to construct a porous adsorption layer. Additionally, a TiO_2 layer is coated onto the surface of the glass fiber to enhance electrostatic adsorption capabilities and strengthen adsorption of viruses or bacteria. Simultaneously, in the presence of light, the TiO_2 layer autonomously performs sterilization and disinfection. After prolonged use, methods such as burning and baking are employed to eliminate organic substances like bacteria or viruses, thus ensuring the complete revived of the inorganic mask.

2. Research Content and Results

2.1 Selection of Glass Fiber

Glass fibers possess a fine fibrous structure, rendering them highly efficient in filtering airborne particulates. However, to fabricate an effective mask filtration layer using glass fibers, it is imperative to ensure their capability to filter out viruses, bacteria, and particulate matter from the air. Consequently, among the commercially available glass fiber sizes (0.22 μm, 0.3 μm, 0.45 μm, 0.8 μm), we opted for the smallest pore size of 0.22 μm as the foundational material for the mask support layer. Considering the necessity of achieving full facial coverage when crafting mask filtration layers from glass fibers, we selected the largest diameter specification among all available

options (25 mm, 47 mm, 50 mm, 90 mm, 100 mm, 150 mm), which is 150 mm.

2.2 Preparation of TiO_2 and Nb-Doped TiO_2 Films

2.2.1 Chemicals for Synthesis

Tetrabutyl titanate ($Ti(OC_4H_9)_4$, ⩾99.0%), acetate ($C_2H_4O_2$, ⩾99.8%), and triethanolamine ($C_6H_{15}NO_3$, AR) were purchased from Aladdin. Ethanol (CH_3CH_2OH, ≥ 99.5%) was purchased from Tianjin Fuyu Fine Chemical Co., Ltd. Rhodamine B ($C_{28}H_{31}ClN_2O_3$, 96%) was purchased from J&K Scientific Co., Ltd. Glass fiber was purchased from Shanghai Xinya Purification Device Factory (Aperture 0.22μm, diameter 150 mm). Deionized (DI) water (resistivity: 18.3MΩ cm) was used for the preparation of aqueous solutions.

2.2.2 Synthesis of TiO_2

The preparation process of nano-TiO_2 film with tetrabutyl titanate as titanium source and anhydrous ethanol as solvent is as follows:

① At room temperature, 5mL tetrabutyl titanate ($Ti(OC_4H_9)_4$) and 17.5mL ethanol (denoted as solution A) were mixed and stirred for 1.5-2 hours until tetrabutyl titanate ($Ti(OC_4H_9)_4$) is dissolved in ethanol. (If the dissolution is not effective, consider adding a surfactant like CTAB and then stir magnetically).

② Gradually add a mixture solution of 17.5 mL of chelating agents (CA) such as acetic acid ($C_2H_4O_2$) or triethanolamine (CH_2CH_2OH) and 0.5 mL of deionized water (denoted as solution B) into the previously stirred mixture of tetrabutyl titanate and ethanol. Maintain uniform stirring during this process.

③ Let the mixture stand for 0.5-1 hour to obtain a uniformly pale-yellow, transparent titanium dioxide sol. Appropriately add 1-1.5 the sol volume of ethanol to adjust the viscosity.

④ Slowly drop the ethanol solution of tetrabutyl titanate into the glass fiber film. Ensure even distribution to cover the entire surface of the glass fiber membrane, so that the internal bubbles are extruded and the titanium dioxide sol penetrates as far as possible, then dry the film for 1.5-2 hours under the indoor temperature.

In this process, the ethanol solution of tetrabutyl titanate gradually undergoes a hydrolysis reaction, leading to the precipitation of $TiO(OH)_2$ gel-like material. Ethanol serves to dilute the reactants, restraining the occurrence of the hydrolysis reaction, thereby slowing down the reaction

rate and ensuring a more uniform precipitation of the gel-like substance. The gradual evaporation of ethanol results in the formation of a gel film while maintaining the integrity and flatness of the gel film during the condensation reaction. A gel is a colloidal system with solid properties, composed of a three-dimensional network structure formed by tiny particles and a continuous dispersed phase.

During the condensation reaction, the gradually formed polymers or particle aggregates connect with each other to form a three-dimensional network structure. During aging, colloidal particles gradually aggregate, ultimately forming a continuous solid network and solidifying into a gel, signifying the basic completion of the reaction.

In subsequent steps, one can opt for the accumulation of titanium dioxide film through static aging or prepare titanium dioxide aerogel and titanium dioxide powder through heating. It's important to note that when preparing the gel, the extended heating time should be maintained below 100°C to prevent the aggregation of TiO_2 nanoparticles during the crystallization process. Finally, the titanium dioxide gel is aged, subjected to immersion and washing treatments, and then dried. After complete precipitation, the solution is allowed to age through static storage.

⑤ The resulting dry matter is treated in the 450℃ and 850℃ heating furnace for 3-4 hours to obtain titanium dioxide film, modified on the glass fiber surface.

2.2.3 Synthesis of Nb-Doped TiO_2

After successfully validating the fundamental sol-gel method for the preparation of titanium dioxide films, we proceeded to further modify TiO_2 through Nb doping. The introduction of Nb^{5+} serves multiple purposes as it introduces defect energy levels through doping, enhancing visible light absorption and introducing electron trapping sites within the TiO_2 lattice, thus more effectively stabilizing holes and improving photocatalytic activity.

The specific procedure involves repeating the aforementioned steps ①-⑥, but replacing the deionized water in step ② with a 3.7 mL solution of niobium oxalate (with a water content of 0.34 mL). Subsequent steps remain unchanged, resulting in the production of Nb-doped TiO_2 thin films.

Note: Niobic acid should be dissolved in water first before mixing it with other components such as tetrabutyl titanate and ethanol to prevent phase separation issues.

2.3 Experimental Results and Discussion

2.3.1 Sol-Gel Coating Methods

In step 2, a chelating agent (CA) such as acetic acid ($C_2H_4O_2$) or triethanolamine (CH_2CH_2OH)

mixed with deionized water (referred to as solution B) is slowly added dropwise into the stirred mixture of tetrabutyl titanate and ethanol (referred to as solution A). It is worth noting that when the mass of solution B added is less than that of solution A, in most cases, the resulting gel has excessively high viscosity, making it unsuitable for film formation and only suitable for verifying the phase transition during calcination.

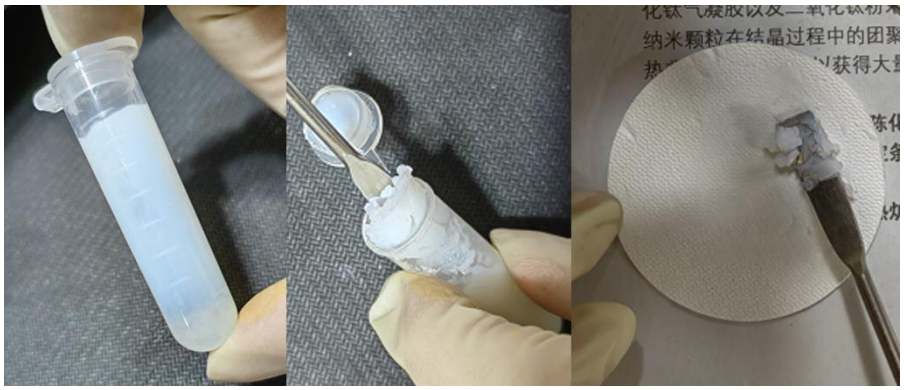

Figure 6. When the mass of solution B added is less than that of solution A, the resulting gel exhibits excessively high viscosity, rendering it impractical for film coating

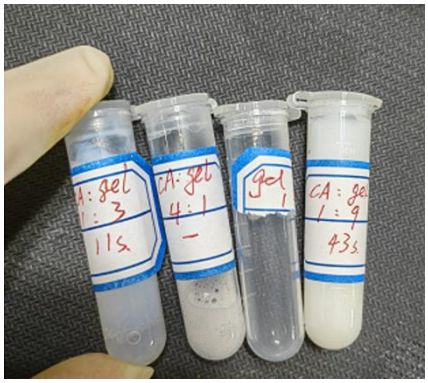

Figure 7. When the ratio of solution B to solution A exceeds 4:1, a relatively thin solution is formed

Experiments have revealed that when the ratio of solution B to solution A exceeds 4:1, a relatively dilute solution is formed, which can be used for subsequent film coating. Additionally, if only the sol prepared in step 1, obtained by mixing 5 mL of tetrabutyl titanate ($Ti(OC_4H_9)_4$) with 17.5 mL of ethanol (referred to as solution A) and stirring for 1.5-2 hours at room temperature, is employed, it can also be used for film deposition. This is because the sol rapidly forms a film due to its reaction with water in the air.

2.3.2 Formula Optimization on Solvents

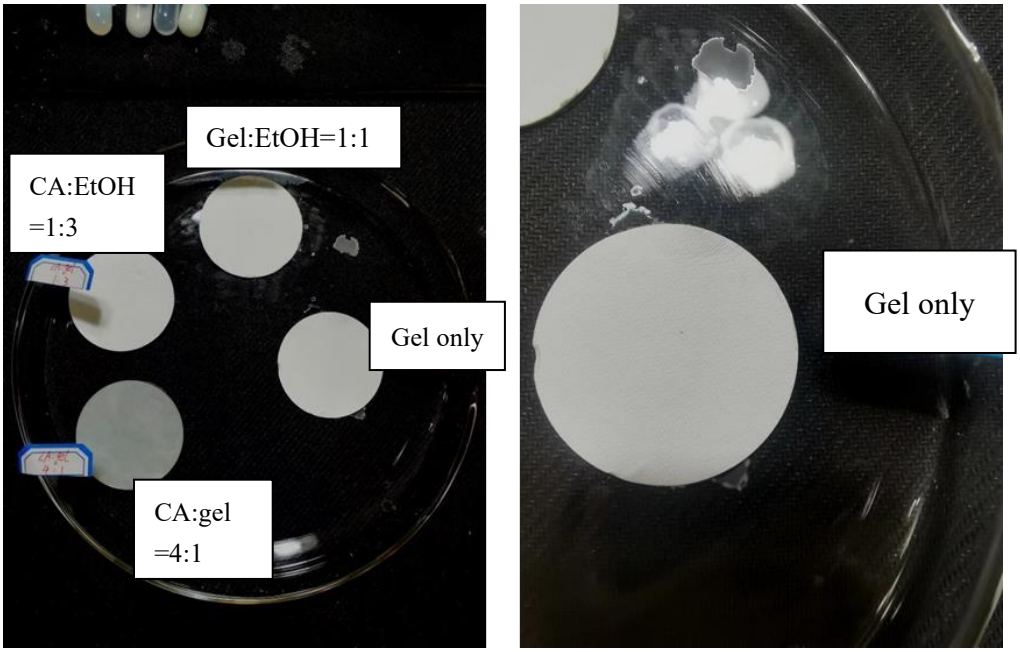

Figure 8. The morphology of sol solution (solution after magnetic stirring of tetrabutyl titanate ethanol, in which the chelating agent drops at a rate greater than or equal to 3ml/min) after being applied or dropped on the surface of glass fiber membranes

When the dosage of chelating agent B (CA) in solution is smaller than that of solution A, it results in the formation of the mentioned condensed gel, leading to solid blockage and making it unsuitable for coating. However, pure solution A or a system with the addition of 1:1 volume ratio (2 ml: 2 ml mixed) of anhydrous ethanol appears as a transparent liquid and can be drop-casted onto the glass fiber surface. At this point, fibrous protrusions appear on the glass fiber surface, and the gloss after solution absorption is brighter than without the addition of ethanol. When chelating agent B exceeds the amount of solution A (represented as CA:gel=4:1), it also exhibits a liquid form (with a significant amount of white turbid liquid) and shows stronger permeability, as shown in Figure 8.

Figure 9. The dripping effect of the original system solution with equal proportion of anhydrous ethanol, which is obviously different from the dripping effect of pure solution.

2.3.3 Crystal Structures after Calcination

Taking into consideration the sintering time and temperature during the calcination process, it is observed that they can have an impact on the phase transition of TiO_2. As the temperature increases and the sintering time extends, TiO_2 nanomaterials gradually crystallize, thereby influencing their photocatalytic activity. Therefore, a study on calcination conditions was conducted.

1) Characterization methods

X-ray Diffractometer (XRD, Shimadzu -6000) was used for phase analysis of the powder materials, and Scanning Electron Microscopy (SEM, Zeiss supra-55) was used to characterize the morphology and particle size of the materials. High Resolution Transmission Electron Microscopy (HRTEM, JEM-2100) was used to characterize the crystal structure of the material, and Ultraviolet-Visible spectrophotometer (Shimadzu, UV-2600) was used to quantify the RhB content, thus analyzing the photocatalytic effect.

2) Characterization Results

In order to avoid the influence of substrates, the dry powder materials, not loaded onto the substrates, were subjected to calcination at 450°C and 850°C, respectively. The crystal phases of TiO_2 were characterized using XRD. The results showed the formation of rutile phase TiO_2 catalyst after calcination at 450°C (Fig.10). The sol-gel method obtained particles with a size of around tens of nanometers (Fig.11), consistent with previous literature reports.

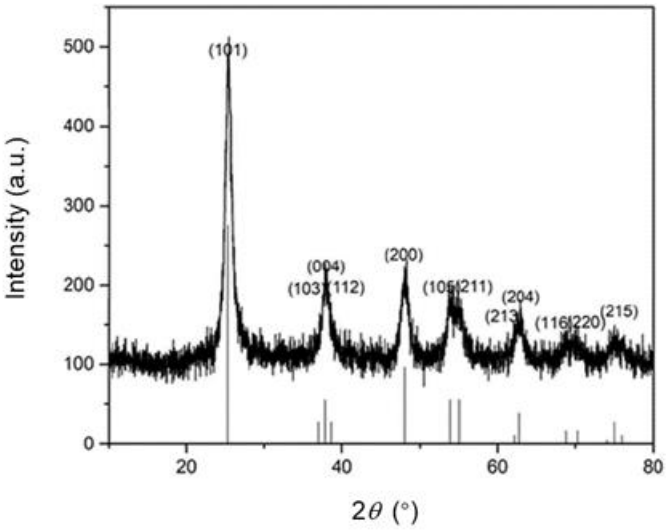

Figure 10. XRD pattern of anatase phase TiO_2 catalyst after roasting at 450℃

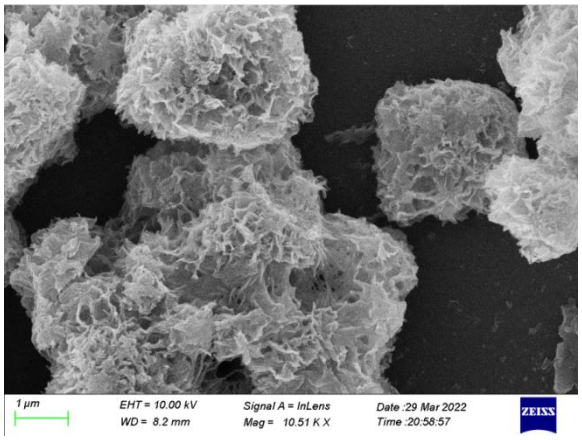

Figure 11. Scanning electron microscopy TiO_2 catalyst after roasting at 450℃

If the temperature is further increased to 850 ℃, the rutile phase TiO_2 catalyst is obtained (Figure 12), which corresponds to the standard card PDF#21-1276.

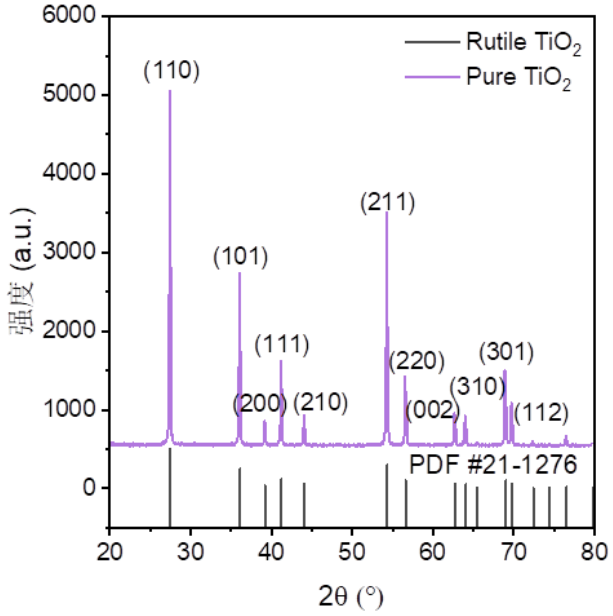

Figure 12. XRD pattern of rutile phase TiO_2 catalyst after roasting at 850℃

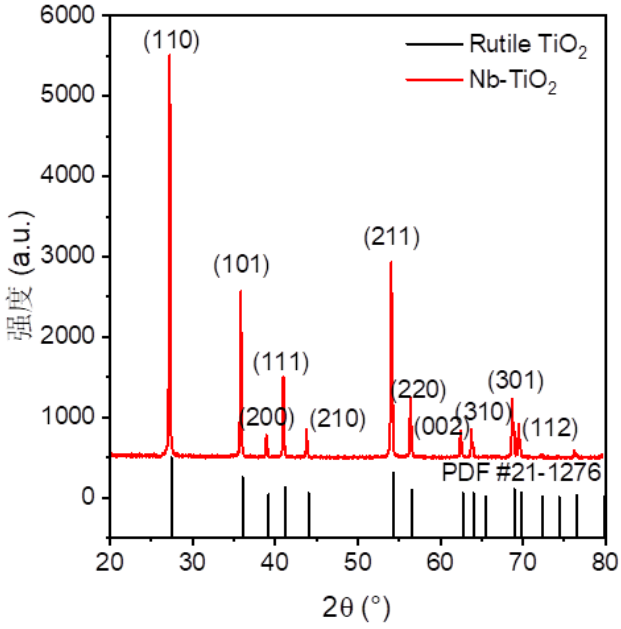

Figure 13. XRD pattern of rutile phase Nb-doped TiO_2 catalyst after 850℃ calcination

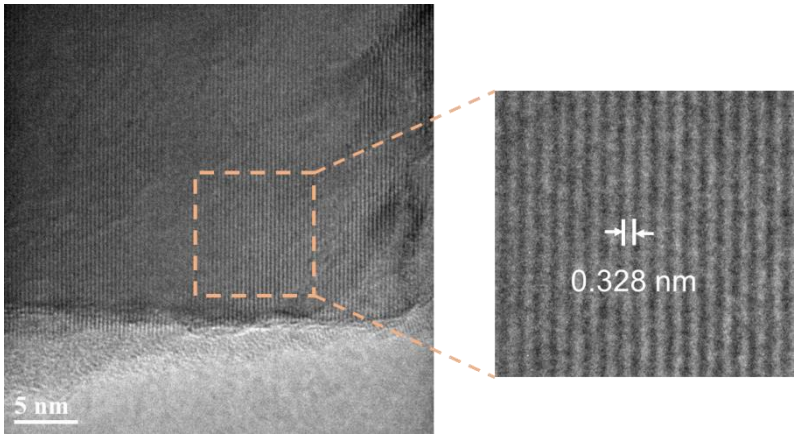

Figure 14. High-Resolution Transmission Electron Microscopy of Nb-doped TiO_2 catalyst after 850 ℃ calcination (Nb doping: 7%)

The TiO_2 prepared by doping Nb has a pure rutile structure without impurity peaks after roasting at 850 ℃ (Figure 13). High-resolution electron microscopy showed that the prepared samples had a relatively perfect regular crystal structure (Figure 14).

2.4 Optimize TiO_2 Coating on Glass Fiber Paper

2.4.1 Comparison and Strategies

1) Uniformity of coating:

Since the uniformity of the drop type coating method in 2.3 cannot be guaranteed, and considering that the ethanol solution of tetrabutyl titanate is gelatinous or not suitable for coating operation, other coating methods are tried.

2) Post-roasting characterization:

Due to the varying thickness of titanium dioxide distribution, the final products after calcination exhibit different degrees of yellow coloration (resulting from light absorption due to defect energy levels in the bandgap), which visually reflects the insufficient uniformity of the coating. Therefore, it is necessary to validate the differences in coating effectiveness among various methods through comparative analysis.

2.4.2 Updated Coating Method

1) Spray coating

A stainless-steel spray gun (BlueMed 116 model gun, 5cc capacity) was selected, and a vacuum heating plate was used as the spraying substrate (0.3mm diameter), as shown in Figure 15. An ethanol solution of tetrabutyl titanate was loaded, and a spraying rate of 5mL per coating was applied

for two consecutive coatings, with each coating distance being ≤15mm. The solution was evenly sprayed onto the rough surface of the glass fiber with a mass of 1.21g , ensuring a coverage thickness of approximately 0.20mm per square centimeter. The coated product (referred to as Product A) was weighed to verify an increase in mass (an ideal weight gain of approximately 1.89-1.92g).

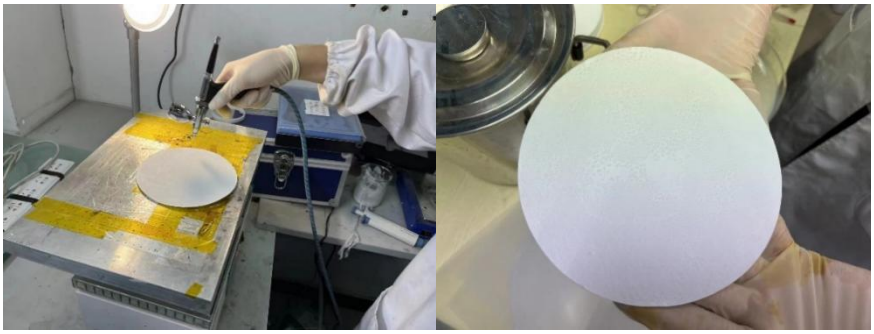

Figure 15. The dry-cleaned glass fiber is sprayed and coated, during which the clear spraying equipment is changed 3 times

2) Wrap and cover

In a wide-mouth glass dish with a diameter exceeding that of the glass fiber (>15cm), an ethanol solution containing tetrabutyl titanate (approximately 5mL) was carefully poured to ensure its even distribution and complete coverage across the dish's base surface, forming an extremely thin layer of solution, measuring less than 0.3mm. After a brief interval of 2 seconds, the clean and dry rough surface of the glass fiber was positioned facing downwards onto the glass cover, gently pressing it to allow the solution to infiltrate the surface without fully penetrating the glass fiber. Following an approximate duration of 10 seconds, the film was peeled off, and this entire process was repeated twice. Finally, the film was left to air dry for 30 seconds to ensure complete surface dryness, ultimately resulting in the production of the final product, referred to as Product B.

2.4.3 Comparison of Products After Calcination

The products A and B were simultaneously subjected to 1.5 hours of calcination at 450°C in a muffle furnace, resulting in the final products shown in Fig. 16. Analysis of the products obtained after calcination, as shown in Fig. 16, clearly reveals a higher distribution of yellow-black spots on product A obtained by spray coating, indicating a lesser coverage compared to product B obtained by encapsulation. The white glass fiber portion is more exposed in product A, demonstrating a more uniform and even coating with minimal agglomeration, hence indicating a more complete oxidation. This uniform coverage of titanium dioxide nanofilm, with lesser structural impact from temperature, results in fewer traces after the combustion of organic compounds. Therefore, the spray coating

method exhibits advantages over the encapsulation and solution dripping methods.

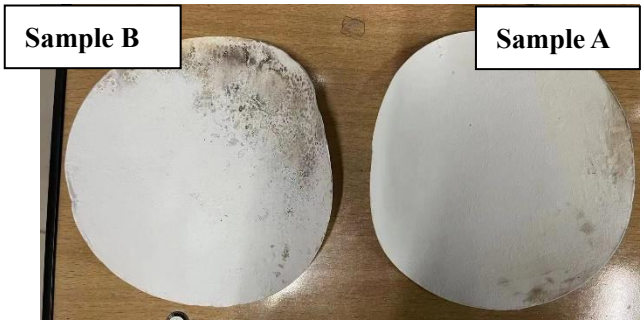

Figure 16. Product A obtained by spray coating (on the right) exhibits fewer yellow-black spots in its distribution, while product B obtained by coating (on the left) shows more black spots.

The obtained products A and B were characterized using scanning electron microscopy (SEM) to examine their interfacial conditions and surface morphology, particularly the dispersion of titanium dioxide (TiO_2) (Fig. 17). From the image, it can be observed that the sample A prepared by the spray coating method exhibits a more uniform distribution, consistent with the visual observations. On the other hand, sample B obtained through the encapsulation method shows localized enrichment of TiO_2 particles.

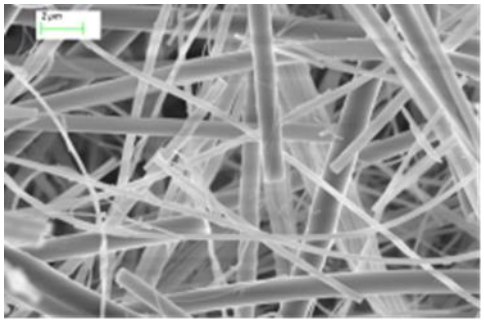

Figure 17-1. SEM image of uncoated smooth fiberglass

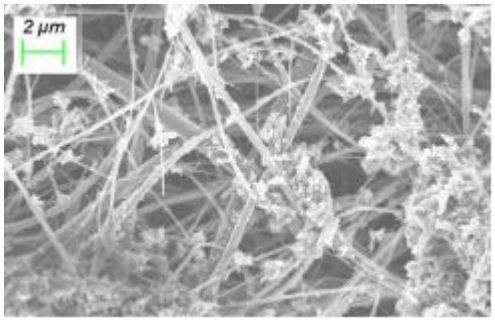

Figure 17-2. SEM image of sample A obtained by spraying method showed that the distribution of TiO_2 particles was relatively uniform

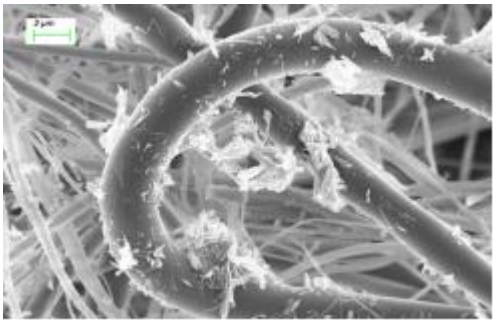

Figure 17-3. SEM image of sample B obtained by parcel overlay method, local enrichment of TiO_2 particles

2.5 Photocatalytic and Antibacterial Activities of TiO_2 and Nb-TiO_2

2.5.1 Photocatalytic Performance of TiO_2 and Nb-TiO_2

1) Measure standard curve.

A. Selection of standard liquid concentration:

When preparing the standard curve, the concentration selection of the standard liquid should generally include the lowest and highest possible variation values of the sample to be tested, and five concentrations can generally be selected. It is best to multiply the concentration gap or increase the grade, and should be measured under the same conditions as the liquid being measured.

B. Determination of standard liquid:

In the color comparison, read the optical density at least 2-3 times to find its average value, in order to reduce the error caused by the instability of the instrument.

C. Drawing of standard curves:

Generally used is the optical density concentration standard curve.

① Use ordinary square paper for drawing. The drawing is best square (length: width=1: 1) or rectangle (length: width =3:2), with the horizontal axis as the concentration, the vertical axis as the optical density, the general concentration of the range of the number of cells, the range of optical density should also occupy the same number of cells. In the appropriate range of preparation of a variety of different concentrations of standard liquid, to obtain its optical density, draw a standard curve, the concentration position to extend upward, the optical density position to the right extension, the intersection point is this coordinate punctuation. Then, the coordinate points and the origin are connected into a line, if it conforms to Lambert-Beer's law, it is a straight line through the origin.

② If the points are not in a straight line, you can pass through the origin, as far as possible to

make the line through more points, so that the points not on the line as evenly distributed on both sides of the line.

③ After the standard curve is drawn, the name of the experimental project, the model and instrument number of the colorimeter used, the filter number or the wavelength of the monochromatic light, and the date and room temperature of the drawing should be indicated on the coordinate paper.

④ Drawing standard curve: it should generally be measured twice or more than three times in parallel, and the curve with good repeatability can be applied.

⑤ The standard curve drawn can only be used for the determination of the same substance under the same conditions. When the instrument is replaced, the position of the instrument is moved, the reagent is changed and the room temperature is changed significantly, the standard curve needs to be redrawn.

⑥ The scale of the horizontal coordinate of the standard curve: convert the content of the standard liquid into the concentration of the liquid to be measured.

According to the above method, the absorption spectrum of Rhodamine B solution measured on the UV-visible spectrophotometer (Shimazu ultraviolet UV-2600) (Figure 18, left) and the standard curve (Figure 18, right) are shown in the Figure 18:

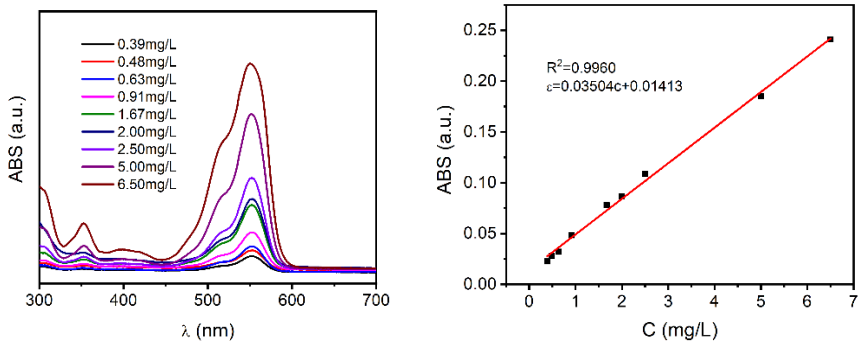

Figure 18. Absorption spectrum and standard curve of Rhodamine B solution

2) Photocatalytic activity test

Test method of photocatalytic activity: 20mL Rhodamine B (Rh B) aqueous solution with a concentration of 6.5mg/L was added to the photoreactor, 10mg photocatalyst was added, and the photocatalyst was stirred for 20h to achieve adsorption-desorption equilibrium on Rh B (marked as -1200 minutes on the figure);

During the activity test, xenon lamp was used as the light source, and samples were taken every

10min after the light was turned on, each sample was 1mL, and the absorbance was tested after centrifugal treatment.

Test data of photocatalytic activity: The photocatalytic activity curves of titanium dioxide (TiO_2) samples calcined at 450 ℃ and NB-doped titanium dioxide (Nb- TiO_2) samples obtained according to the above test methods are shown in the figure 19:

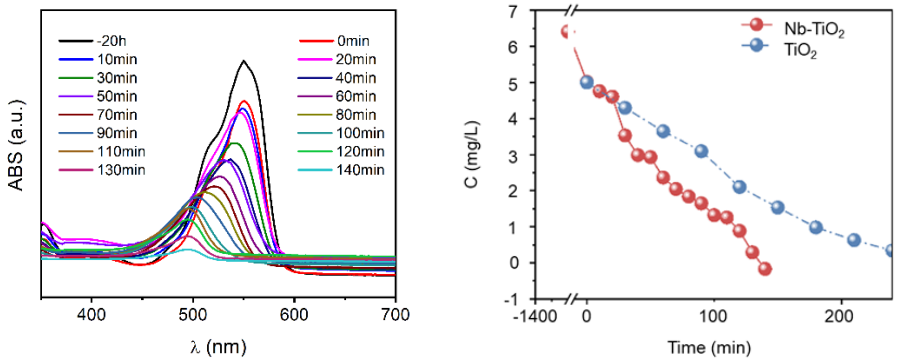

Figure 19. Left: Light absorption spectra of Rhodamine B solution obtained by Nb-TiO2 sample for photocatalytic activity test; Right: comparison of photocatalytic activity of TiO_2 and Nb-TiO_2 samples

3) Analysis of photocatalytic activity test data

The above comparison of photocatalytic data shows that Nb doping has better photocatalytic activity than undoped pure TiO_2 under the same conditions, proving that doping TiO_2 with high-priced (5+) Nb is an effective means to improve photocatalytic activity, showing its potential application in photocatalytic sterilization and other aspects.

2.5.2 Principles and Methods of Photocatalytic Antibacterial Performance Testing

1) Photocatalytic sterilization test method

Photocatalytic bactericidal performance is basically carried out by ISO 27447:2019 standard test method. It is mainly by measuring the number of bacteria after exposure to a certain ultraviolet (UV) or visible light irradiation, to determine the bactericidal activity of materials containing photocatalysts or having a photocatalytic film on the surface. Both solids (non-porous) and textiles can have a photocatalyst or have a photocatalytic film, and can be tested using the ISO 27447:2019 standard method by examining the number of microorganisms that may be present on the surface after exposure to light, ultraviolet light.

The specific steps include: prepare 500 mL liquid medium, pour into 10 bottles of 50 mL each, cover with a semi-permeable film, hold with a rope or rubber band, and culture the liquid medium

under the premise of ensuring light and air permeability: fill the surface of the sample as the base, and inoculate the bacteria on the test and control surfaces. Additional bacterial strains can be requested, the sample is exposed to ultraviolet or visible light for a period of time, and then live bacteria are extracted from the test and control materials and counted

2) Photocatalytic bactericidal test results with discussion:

Escherichia coli and Staphylococcus aureus were used as test strains, LED lamp was used as light source (light intensity 5.62 mW/cm²), and sterilization tests [14-15] were carried out on blank glass fiber, TiO_2 loaded glass fiber, and Nb-TiO_2 loaded glass fiber under visible light.

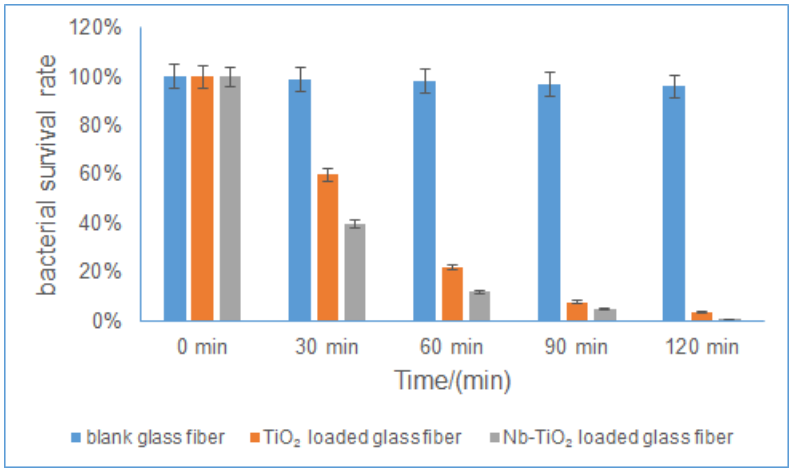

Figure 20. Comparison of bactericidal performance of glass fiber (blank pair,blue), TiO_2 loaded glass fiber (undoped sample, orange), and Nb-TiO_2 loaded glass fiber (best sample, gray)

The three types of materials exhibit very different bactericidal properties. Among them, the blank glass fiber hardly showed any obvious photocatalytic bactericidal activity under visible light.

Glass fibers loaded with TiO_2 showed excellent bactericidal properties, as shown in Figure 20. The bactericidal effect of 40% was achieved within 30 minutes. This means that if we wear such a mask to go out for more than half an hour, it can basically have an obvious bactericidal effect under general lighting conditions. Over time, the photocatalytic mask loaded with TiO_2 further improves its bactericidal effect under visible light irradiation, reaching a bactericidal rate of 78% and 92% at 60 minutes and 90 minutes, respectively, which means a bacterial survival rate of 20% and less than 10%. When the irradiation time was extended to 2 hours, the bactericidal rate of the composite fabric reached more than 96%, and the bactericidal effect was obvious.

The glass fiber loaded with Nb-doped TiO_2 showed better bactericidal performance (Figure 20.).

60% bactericidal efficacy (40% survival) was achieved within 30 minutes. Approximately 50% improvement over TiO_2 only loaded (undoped sample). With the extension of time, the photocatalytic bactericidal effect of loaded niobium doped TiO_2 was further improved, reaching 88% and 95% bactericidal rate in 60 minutes and 90 minutes, respectively. When the irradiation time was extended to 2 hours, the bactericidal rate of the composite fabric was more than 99%, and the bactericidal effect was very obvious.

The above characterization data of photocatalytic bactericidal performance show that Nb doping has better photocatalytic bactericidal activity than undoped pure TiO_2 under the same conditions, which proves that doping TiO_2 with high price (5+) Nb is an effective means to improve bactericidal activity, and confirms its application in photocatalytic bactericidal activity.

2.6 Filtration Efficiency Test

2.6.1 Testing Sample Preparation

In order to facilitate the compliance of the surface area requirements of the glass fiber filter layer and the guarantee of structural stability during the filtration test, the product A and B are hot pressed, the specific steps are as follows:

① Select the purchased PVC transparent plastic film, cut the thickness of about 0.1mm film, the product A, B sandwiched in two films of the same size, so that it into A three-layer structure, this method is repeated 4 times, so that the upper, lower, left and right directions of the product A, B are basically covered, leaving the middle of 10cm×10cm without coverage for filtration test.

② The covered product is sent to the hot press (fuel cell special press, maximum pressure 100Kg/mm2, power 3.1KW) hot pressing, data testing and repeated experiments, the highest pressure of 0.3MPa, temperature 130-145℃ hot pressing for 15min, can make PVC components melt cover the product, And ensure that the glass fiber is not broken by pressure resulting in product damage.

③ After hot pressing, take out the product and stand for 10min.

2.6.2 Mask Filtration Efficiency Testing

Test the mask filtration performance of products A and B after hot pressing, select a mask filtration performance tester (SC-FT-1702DYY mask filtration performance tester), and perform a rapid measurement of NaCl aerosol filtration for each product, each rapid measurement lasts for 15s, and record the filtration efficiency, flow rate and corresponding resistance. The average value of

each data was recorded for 3 consecutive times.

The average data obtained are recorded as follows, where the thickness of pure glass fiber is about 0.3mm (the same as that of products A and B):

Table 1: Summary of Glass Fiber Membrane Filtration Performance Test Results

	Product A	Product B	Pure fiberglass
Filtration efficiency %	98.82	96.72	99.73
Resistance /Pa	316.67	316.03	311.17
Flow L/min	32	32	32

Note: Due to the same test source, the traffic data of each test object is consistent

Figure 21. Perform a mask filtration test

Based on the filtration experiments, the following conclusions were drawn:

1) In comparison to pure glass fiber as a reference, the filtration efficiency of product A (obtained through spray coating) is affected by the coated film. It exhibits a slight decrease in fiber filtration efficiency relative to pure glass fiber, accompanied by a certain increase in resistance (approximately 5 Pa).
2) The filtration efficiency of product B (obtained through encapsulation) decreases due to uneven coating and areas with excessive thickness. Additionally, its resistance fluctuates significantly due to the uneven surface (corresponding to 321.8 Pa/319.2 Pa/307.1 Pa, with a fluctuation range of approximately 14 Pa).

When compared to other masks currently in use in society, the data regarding the filtration layer of the developed inorganic mask (with reference to product A) shows that its resistance is lower than medical protective masks like N95, while still meeting the filtration efficiency requirements.

However, the resistance is much higher than that of medical surgical masks (common household masks). Therefore, if the objective and main focus of the product's development is for regular use, adjustments and improvements need to be made to factors that affect resistance, such as opting for thinner glass fiber membranes.

2.6.3 Consideration on Filtration Efficiency Improvement

At present, the adjustment and improvement of the resistance reduction of the mask filter layer (that is, products A and B) focus on reducing the thickness of the glass fiber substrate. The main method to consider and adopt is to buy a thinner glass fiber film (thickness ≤0.3mm, but it cannot guarantee the corresponding mechanical strength and hardness), and also consider the way of manual reduction. Including using transparent tape to stick and adsorb glass fiber, repeated operation to reduce its thickness, etc., limited by the lack of materials and the uncertainty of the experiment, no relevant tests were conducted

2.7 Mask Regeneration under High-Temperature

2.7.1 Removal of Organic Residue by Calcination

Although the method of photocatalysis can kill bacteria, the working principle of this kind of sterilization is that under the action of photocatalysis, the epidermis of the bacteria is destroyed and the activity is lost. The body of the bacteria is still attached to the surface of the catalyst, preventing the future work of TiO_2 and Nb-TiO_2. Therefore, after a period of use, it is necessary to use high temperature treatment to revive the mask.

Specific steps:

1) Select product A and cut it, cut it into two 5cm×10cm rectangular filter membrane (recorded as α membrane and β membrane), weigh it and record it. The weight of α film and β film was about 0.34g. After that, coffee coloring was added to the surface respectively (10mL powder mixed with 90mL water mixed solution), about 10 drops were uniformly added to the α film with the dropper of the glue head, and a total of about 7mL mixed solution was non-uniformly sprayed on the β film, which was weighed and recorded after standing for 3min. The weight of α film is about 0.52g, and the weight of β film is about 0.75g.
2) The α film and β film were sent into the Muffle furnace, 450℃ was selected as the upper temperature for roasting, 5min was taken as the cycle time node, and the exposure of coffee traces was periodically recorded.

3) After about 30min, the α film and β film were removed from the Muffle furnace, and were respectively weighed after 1min. The weight of the α film was about 0.35g, and the weight of the β film was about 0.39g.

The periodic recording chart is as follows:

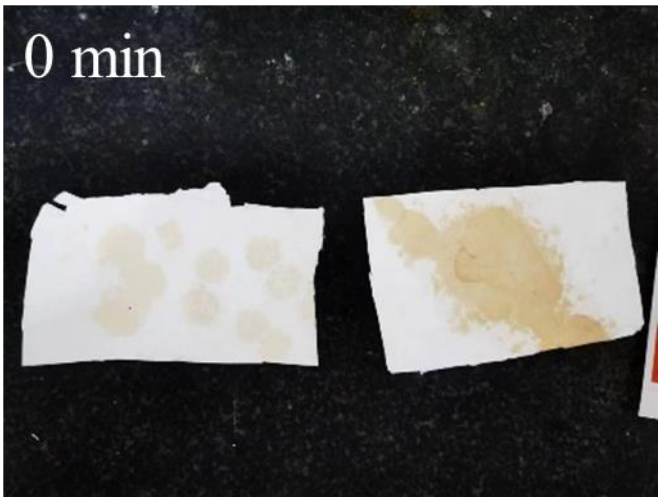

Figure 22. Initial state (left for α membrane, right for β membrane)

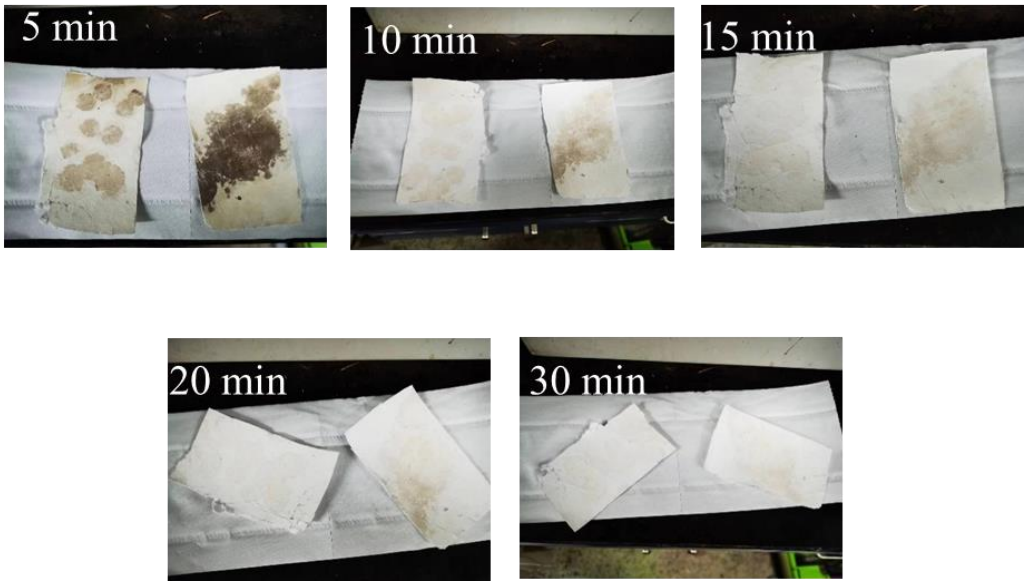

Figure23. Periodic recording (5min is the recording interval, a total of 30min)

As it shown in Figure 22 & 23, the organic component pollution (coffee) on the surface of the filter membrane can be basically removed under the roasting environment of 450℃ for about 30min. By comparing the quality changes before and after the pollution, it is confirmed that the high-temperature roasting resurrection has no effect on the inorganic filter membrane itself, and can still be used after roasting without structural damage, powder loss, film breakage, etc. At the same time,

the characteristics of high temperature resurrection were also verified. For other smaller residues of organic matter (bacteria, viruses, etc.), the efficiency of high temperature removal is faster, the effect is better, and the temperature requirement is relatively lower.

2.7.2 Proposal on Standard High-Temperature Regeneration

There are two ways of high temperature sterilization: dry heat sterilization and wet heat sterilization. Dry heat treatment includes: dry heat 135 ℃ ~145 ℃ sterilization for 3-5 hours; 160-170 ℃ sterilization for 2-4 hours; 0.5- 1 hours for sterilization at 180-200 ℃, etc.; Humid heat 134 ℃ for hospital use only. In fact, microwaves can kill bacteria. But these methods generally do not completely remove the bacterial shell. For the formulation of the relevant reanimation standards, the environment is a domestic iron pan, and the method is to directly "dry fry" the film in the iron pan.

The specific steps include:

1) The iron pan (note that there can be no film, especially the non-stick pan cannot, PTFE will decompose due to high temperature) wash and dry, placed on the gas stove, point a small fire with an external flame to heat.
2) The glass fiber that is slightly yellow due to long-term use is spread flat on the bottom of the pot, about 15 seconds after turning the page, until both sides show a significant increase in white, that is, it is advisable to cool down. Can be used again after 5-10min cooling, pay attention to the preservation of the environment as far as possible to ensure cleanliness.
3) Considering that there may be new bacteria attached during the cooling process, the distribution of bacteria after "dry frying" was not detected here, and only the color was used as a reference. Considering that the ignition point of general carbohydrates (such as starch) is below 400oC, this method has great universality and application potential.

3. Innovation Points and Conclusions

The project presents the following three main innovations:

1) The use of a glass fiber membrane instead of a polymer membrane for filtration, providing the "rebirth from fire" characteristic for masks. This involves complete revival of inorganic masks through high-temperature heating, enabling their long-term use.
2) Utilizing glass fiber as a framework with a surface-coated TiO_2 nanofilm, which enables photocatalytic degradation of viruses or bacteria, thereby achieving self-cleaning under light

irradiation.

3) The introduction of Nb doping to induce defect energy levels, enhancing visible light absorption and introducing electron capturing sites in the TiO_2 lattice, which contribute to more effective stabilization of holes and improvement of photocatalytic activity.

Relevant research conclusions of this project:

1) The feasibility of "inorganization" of masks has been verified, along with its advantages over organic masks in certain aspects.
2) The feasibility of the "sol-gel combined with spray coating" method for producing TiO_2 coatings on glass fiber substrates has been confirmed.
3) The enhancement of photocatalytic activity in titanium dioxide through niobium doping has been validated and applied to sterilization.

4. Prospects of the Project

Figure 24. Shortcomings and improvement plans of fiberglass masks

In spite of the advantages we mentioned above, we still worry about the following limitations, and consequent solutions are also proposed for future improvements:

1) While using glass fiber as a framework offers the advantage of high-temperature resistance, it also raises some concerns worth discussing and addressing, such as potential respiratory hazards. Fine glass fibers that enter the lungs through respiration cannot be absorbed or broken down, leading to lung damage and potential health issues like silicosis. Workers exposed to high concentrations of glass fibers may also experience bronchitis, upper respiratory tract irritation, and asthma.

   Future solutions: Adopt a double-layered structure with an externally exposed TiO_2-loaded glass fiber membrane and an inner layer made of polymer PP fibers. The polymer membrane acts as a barrier to prevent glass fibers from entering the lungs. Additionally, incorporate a flat

membrane tile structure similar to industrial masks to prevent glass fiber breakage. (Figure 24, left image)

2) The framework obstructs the photocatalytic process by blocking the light from reaching the catalyst.

   Future solution: Utilize a transparent framework. Since the heated portion that is dismantled is only the surface inorganic filtration membrane, other parts can still be made of polymer materials in a transparent structure (Figure 24, right image).

3) The glass fiber membrane tends to be hydrophilic, leading to water flooding during respiration and reduced breathability.

   Future solution: Incorporate a breathing valve structure. Excessive moisture inside the mask during exhalation is the main cause of water flooding, so the use of an exhalation valve allows the exhaled gas to bypass the glass fiber membrane, greatly reducing the likelihood of water flooding.

5. Acknowledgement

I appreciate Prof. HUANG Yaqin for giving the kind instructions and providing experimental conditions, Master student GAO Wenqin for preparing chemicals for experiments and kind advice, Prof. HU Shui for helping on filtration property evaluation.

6. References

[1]. Taekyu Joo, Masayuki Takeuchi, Fobang Liu, et al. Evaluation of particle filtration efficiency of commercially available materials for homemade face mask usage [J]. Aerosol Science and Technology, 2021, 55(8): 930-942.

[2]. Qiang Li, Yongchao Yin, Daxian Cao, et al. Photocatalytic Rejuvenation Enabled Self-Sanitizing, Reusable, and Biodegradable Masks against COVID-19 [J]. ACS Nano, 2021, 15 (7): 11992-12005.

[3]. Selvakumar Vijayalakshmi, Preethi Gopalsamy, et al. Environmental Hazard of Polypropylene from Disposable Face Masks Linked to the COVID-19 Pandemic and Its Possible Mitigation Techniques through a Green Approach [J]. Journal of chemistry, 2022, 2022:17.

[4]. Yang, W., Cao, L., Li, W. et al. Carbon Nanotube prepared by catalytic pyrolysis as the electrode for supercapacitors from polypropylene wasted face masks [J]. Ionics, 2022, 28: 3489–3500.

[5]. Cui, J., Qi, M., Zhang, Z. et al. Disposal and resource utilization of waste masks: a review [J]. Environ Sci Pollut Res, 2023, 30: 19683–19704.

[6]. Wang, H., Guo, X., Pei, C., et al. Hydrophilic modification of polypropylene membrane via tannic and titanium complexation for high-efficiency oil/water emulsion separation driven by self-gravity [J]. Polym. Eng. Sci., 2022, 62(7): 2131.

[7]. https://oceansasia.org/beach-mask-coronavirus/.

[8]. 任强，李建章，鹿振友.木纤维/岩棉纤维复合材料的研究 [J].北京林业大学学报，2007,02.

[9]. 肖艳.玻璃纤维复合材料的应用[J].模具制造，2013,04:76-80.

[10]. 刘定彪.玻璃纤维及其复合材料的应用进展[J].基层建设，2017,20.

[11]. Zhang, X., Liu, S., Salim, A., Seeger, S., Hierarchical Structured Multifunctional Self-Cleaning Material with Durable Superhydrophobicity and Photocatalytic Functionalities [J]. Small, 2019, 15: 1901822.

[12]. Swagata Banerjee, Dionysios D. Dionysiou, Suresh C. Pillai. Self-cleaning applications of TiO_2 by photo-induced hydrophilicity and photocatalysis [J]. Applied Catalysis B: Environmental, 2015, 176: 396.

[13]. Maria Solovyeva, Dmitry Selishchev , Svetlana Cherepanova et al. Self-cleaning photoactive cotton fabric modified with nanocrystalline TiO_2 for efficient degradation of volatile organic compounds and DNA contaminants [J]. 2020, 388: 124167.

[14]. 杨岳，张敏，关成立. 纳米光催化剂 TiO_2 的结构表征及光催化杀菌性能[J].食品工业科技，2019, 40 (03).

[15] 张丽，刘又年，周民杰.光催化杀菌机理研究进展[J].湖南理工学院学报，2011，24 (03)